

## **CHAPTER 5**

## Chapter 5

### Effect of magnetic field on laminar channel flow driven by accelerating walls

#### 5.1. Introduction

Steady state natural convection flows in vertical channels are of interest in a number of engineering applications. One of these is the natural convection cooling of electronic cabinets containing circuit cards which are aligned to form vertical channels. The importance of heat transfer considerations in the design of electronic equipment has been reviewed by Aung and Chimah (1983) and Jaluria (1985).

The analysis of simultaneously developing laminar flows has been of great interest, as demonstrated by the vast literature available, in connection with a demand for more precise reference data by heat exchanger designers (Shah (1983)). Shah and London (1978) provide an extensive list of contributions related to this class of problems, mostly in simple geometries such as circular tubes, parallel plate channels and annular ducts.

Many diverse flow configurations are of interest in electronic cooling applications. The most important of these configurations is the vertical channel. Laminar, natural convection heat transfer in vertical channels has been investigated theoretically as well as experimentally. Representative contributions to the analytic literature on the subject have

been made by several investigators. Fully developed natural convection flow in a parallel wall channel has been treated for heat transfer by Bodoia and Osterle (1962) for uniform, equal temperature walls and by Ostrach (1952), Aung (1972), Miyatake and Fujii (1972, 1973, 1974) and Miyatake *et al* (1973) for asymmetric heating.

Convection is an important parameter in crystal growth experiments from the melt as it can account for both heat and mass transfer in the liquid phase. It is well known that these unavoidable hydrodynamic movements can be damped with the help of a magnetic field (Vives and Perry (1987); Utech and Flemmings (1966)). The work of Hart (1972, 1983) and Birikh (1966) was extended by Garandet *et al* (1992) to the case where a magnetic field is present. They proposed a two dimensional solution to the equations of the magnetohydrodynamics that can be used to model the horizontal Bridgman method.

In the present analysis we consider a similarity solution of the Navier-Stokes equations which describe the two dimensional flow of a viscous, incompressible, electrically conducting fluid in a channel with accelerating walls. We consider the effect of a uniform, varying magnetic field. Insistence that the flow be of similarity form allows a reduction of the Navier-Stokes equations to two partial differential equations for the stream function in one space dimension. We have used normal mode approach to linear stability. Some results for small Reynolds number are

presented and these asymptotic results are complemented by numerical results about the steady solutions and their instabilities. Asymptotic solutions for large Reynolds number  $R$  are also obtained.

## 5.2. Mathematical formulation

We consider two-dimensional flow of an incompressible electrically conducting, viscous fluid in a channel  $-\infty < x < \infty$ ,  $-h < y < h$  with velocity components  $u, v$  in the  $x, y$  directions. We assume that a varying magnetic field  $\vec{H} = (H_x, H_y, 0)$  is present. The governing system of equations of motion and the continuity equation is given by

$$\nabla \cdot \vec{q} = 0 \quad (5.2.1)$$

$$\begin{aligned} \rho_0 \left( \frac{\partial \vec{q}}{\partial t} + (\vec{q} \cdot \nabla) \vec{q} \right) = & -\nabla p + \rho_0 \vec{F}_g + \mu \nabla^2 \vec{q} \\ & + \mu_e (\nabla \times \vec{H}) \times \vec{H} \end{aligned} \quad (5.2.2)$$

where  $\rho_0$ ,  $\mu_e$ ,  $\mu$  denote respectively the density, magnetic permeability and co-efficient of viscosity of the fluid and  $\vec{q}$ ,  $\vec{H}$ ,  $p$  denote the velocity, magnetic field and pressure of the fluid. Equation of motion for the magnetic field, which express the interactions between the fluid motions and the magnetic fields is obtained as,

$$\frac{\partial \vec{H}}{\partial t} = \eta \nabla^2 \vec{H} + \nabla \times \vec{V} \times \vec{H} \quad (5.2.3)$$

$$\nabla \cdot \vec{H} = 0 \quad (5.2.4)$$

where  $\eta$  is the magnetic resistivity of the fluid.

To complete the system of equations (5.2.1) - (5.2.4) the following boundary conditions are imposed.

$$\begin{aligned} u &= E_1(t) x & v &= V_1(t) & H_y &= 1 & \text{at } y &= h \\ u &= E_2(t) x & v &= V_2(t) & H_y &= 1 & \text{at } y &= -h \end{aligned}$$

To eliminate the equations (5.2.1) and (5.2.4), we introduce velocity and magnetic stream functions

$$\begin{aligned} \vec{q} &= \left( \frac{\partial \psi}{\partial y}, -\frac{\partial \psi}{\partial x}, 0 \right) \\ \vec{H} &= \left( \frac{\partial \psi_m}{\partial y}, -\frac{\partial \psi_m}{\partial x}, 0 \right) \end{aligned} \quad (5.2.5)$$

Hence the stream functions  $\psi$  and  $\psi_m$  satisfy the equations

$$\frac{\partial \nabla^2 \psi}{\partial t} + \frac{\partial (\nabla^2 \psi, \psi)}{\partial (x, y)} = \nu \nabla^4 \psi + \frac{\mu_e}{\rho_0} \frac{\partial (\nabla^2 \psi_m, \psi_m)}{\partial (x, y)} \quad (5.2.6)$$

$$\frac{\partial \psi_m}{\partial t} = \eta \nabla^2 \psi_m + \frac{\partial (\psi, \psi_m)}{\partial (x, y)} \quad (5.2.7)$$

Non-dimensionalisation will be carried out by introducing a velocity scale  $w$  and length scale  $h$ , which are characteristics of the variations of the basic current. We define the dimensionless co-ordinate time, and intensity of the magnetic field as

$$t = ht' / w ; \quad \vec{H} = H_0 \vec{H}' \quad (5.2.8)$$

$w$  is a velocity scale based on  $V_1, V_2, E_1 h$  or  $E_2 h$ . Hence the non-dimensional system of equations, obtained by using equation (5.2.8) in (5.2.6) and (5.2.7), is given by

$$\frac{\partial \nabla^2 \psi}{\partial t} + \frac{\partial (\nabla^2 \psi, \psi)}{\partial (x, y)} = \frac{1}{R} \nabla^4 \psi + S^2 \frac{\partial (\nabla^2 \psi_m, \psi_m)}{\partial (x, y)} \quad (5.2.9)$$

$$\frac{\partial \psi_m}{\partial t} = \frac{1}{R'_m} \nabla^2 \psi_m + \frac{\partial (\psi, \psi_m)}{\partial (x, y)} \quad (5.2.10)$$

where the magnetic pressure number is characterized by  $S^2 = \frac{\mu_e H_0^2}{\rho_0 w h}$ . The Reynolds number  $R$ , a measure of the ratio of inertial force to viscous force and the magnetic Reynolds number  $R'_m$ , a measure of the effect of the flow on the magnetic field are defined as

$$R = \frac{w h}{\nu} \quad ; \quad R'_m = \frac{w h}{\eta}$$

The symmetric case when  $E_1(t)=E_2(t)=0$  with  $V_1(t) = -V_2(t) = \text{constant}$ , was considered by Zaturka *et al* (1988). Cox (1991) considered the asymmetric case when  $E_1(t) = E_2(t) = 0$  with  $V_1(t), V_2(t)$  unequal constants. The symmetric case when  $V_1(t) = V_2(t) = 0$  with  $E_1(t) = E_2(t) = \text{constant}$ , has been considered by Watson *et al* (1990). In the present work, we consider the case when  $V_1(t) = V_2(t) = 0$  but  $E_1(t), E_2(t)$  are unequal and constant. We put  $E_1(t) = E$ , a constant and  $E_2(t) = \alpha E$ . We assume, without loss of generality that  $\alpha$  lies in the range  $[-1,1]$ .  $\alpha$  may be replaced in this range by a simple rescaling. Also we replace  $w$  by  $Eh$ .

The similarity form for the two-dimensional flow may be used when the flow is driven by suction or injection or by accelerating walls or by both mechanisms simultaneously. The similarity form has a long history. It was originally applied by Hiemenz to flow at a stagnation

point. Thus, we seek a similarity solution of equations (5.2.9) and (5.2.10) in the form

$$\psi = x f(y, t, \alpha, R, R'_m, S^2) \quad (5.2.11)$$

$$\psi_m = x g(y, t, \alpha, R, R'_m, S^2) \quad (5.2.12)$$

Substitution of equations (5.2.11) and (5.2.12) in equations (5.2.9) and (5.2.10) yields

$$f_{yyt} + f_{yy} f_y - f f_{yyy} = R^{-1} f_{yyyy} + S^2 (g_y g_{yy} - g g_{yyy}) \quad (5.2.13)$$

$$g_t = \frac{1}{R'_m} g_{yy} + (f g_y - g f_y) \quad (5.2.14)$$

subject to the boundary conditions,

$$f_y = 1 \quad f = 0 \quad g = 1 \quad \text{at } y = 1$$

$$f_y = \alpha \quad f = 0 \quad g = 1 \quad \text{at } y = -1$$

subscripts denote partial differentiation.

The average values of the velocity and magnetic stream functions are decomposed into two parts respectively by  $F(y)$ ,  $G(y)$  and  $\bar{f}(t,y)$ ,  $\bar{g}(t,y)$  where  $\bar{f}$  and  $\bar{g}$  describe small perturbations superposed on the initial variables.

The dependence of the disturbance quantities in dimensionless form is assumed to be  $\exp(st)$ , where  $s$  the phase velocity may be complex.

The steady state solutions correspond to

$$\psi = x F(y, \alpha, R) \quad \text{and} \quad \psi_m = x G(y, \alpha, R)$$

where

$$F^{iv} + R (FF''' - F' F'') - S^2 R (G G''' - G' G'') = 0$$

$$\text{and} \quad G'' + R'_m (FG' - G F') = 0 \quad (5.2.15)$$

with boundary conditions,

$$F(-1) = 0 \quad ; \quad F'(-1) = \alpha \quad ; \quad F(1) = 0 \quad ; \quad F'(1) = 1$$

$$G(-1) = 1 \quad ; \quad G(1) = 1 \quad (5.2.16)$$

This problem, in the absence of the magnetic field was studied by Watson *et al* (1991).

To obtain the equations governing the perturbations, the disturbance quantities are expressed as

$$\bar{f}(t, y, \alpha, R) = e^{st} \phi(y, \alpha, R)$$

$$\bar{g}(t, y, \alpha, R) = e^{st} \lambda(y, \alpha, R)$$

Thus the eigenfunctions and eigenvalues satisfy

$$R s \phi_{yy} + R [F_{yy} \phi_y + \phi_{yy} F_y - F \phi_{yyy} - \phi F_{yyy}]$$

$$= \phi_{yyyy} + S^2 R [\lambda_y G_{yy} + G_y \lambda_{yy} - \lambda G_{yyy} - G \lambda_{yyy}] \quad (5.2.17)$$

$$R'_m s \lambda = \lambda_{yy} + R'_m [\phi G_y + F \lambda_y - \lambda F_y - G \phi_y] \quad (5.2.18)$$

with boundary conditions

$$\phi(\pm 1) = 0, \quad \phi'(\pm 1) = 0; \quad \lambda(\pm 1) = 0; \quad (5.2.19)$$



### 5.3. Small R-analysis of steady solutions

In this section, we attempt to study the effect of small Reynolds number to a laminar channel flow driven by accelerating walls. Hjellming and Walker (1987) conducted an investigation of the effect of an axial magnetic field on the crucible wall boundary layers that occur in the magnetic Czochralski crystal growth technique. The analysis was carried out in the limit of large magnetic interaction number, in which case the nonlinear inertia terms may be neglected. Such a large value of the magnetic interaction number is not always obtained in practice. The approach adopted here is to consider the situation when the magnetic field is weak; however the equations are fully nonlinear and we have to make several simplifying assumptions in order to make progress.

We assume the following asymptotic series for the stability parameter, steady solutions and perturbed solutions:

$$\begin{aligned}
 s &= -R^{-1} s_{-1} + s_0 + R s_1 + \dots \\
 R'_m &= R R_m \\
 S^2 &= R^{-1} M \\
 \lambda &= \lambda_0 + R \lambda_1 + R^2 \lambda_2 + \dots \\
 \phi &= \phi_0 + R \phi_1 + R^2 \phi_2 + \dots \\
 G &= G_0 + R G_1 + R^2 G_2 + \dots \\
 F &= F_0 + R F_1 + R^2 F_2 + \dots
 \end{aligned} \tag{5.3.1}$$

Substituting equation (5.3.1) in equation (5.2.15), and equating the like powers of  $R$ , the equations to be satisfied by the zeroth and first order approximation of velocity and magnetic field are obtained as follows.

$$\begin{aligned}
 F_0^{iv} - M [ G_0 G_0''' - G_0' G_0'' ] &= 0 \\
 G_0'' &= 0 \\
 F_1^{iv} + F_0 F_0''' - F_0' F_0'' - M \{ G_0 G_1''' + G_1 G_0''' \\
 &\quad - G_0' G_1'' - G_1' G_0'' \} = 0 \\
 G_1'' + R_m (G_0' F_0 - G_0 F_0') &= 0 \quad (5.3.2)
 \end{aligned}$$

By solving equations (5.3.2) subject to the boundary conditions

$$\begin{aligned}
 F_n(\pm 1) &= 0; \quad G_0(\pm 1) = 1; \quad F_0'(-1) = \alpha \\
 F_0'(+1) &= 1; \quad G_n(\pm 1) = 1; \quad F_n'(\pm 1) = 0; \quad n \geq 1
 \end{aligned}$$

we arrive at the following steady state solutions

$$\begin{aligned}
 F_0(y) &= \frac{1}{4} (y^2 - 1) [ (1 - \alpha) + (1 + \alpha) y ] \\
 G_0(y) &= 1 \\
 F_1(y) &= (y^2 - 1)^2 \left\{ \left( \frac{1 + \alpha}{4} \right)^2 \frac{1}{70} y (y^2 + 2) \right. \\
 &\quad \left. + \left( \frac{1 - \alpha^2}{4} \right) (y^2 + 7) \right. \\
 &\quad \left. + \left( \frac{1 - \alpha}{4} \right)^2 \frac{1}{30} y + M R_m \left( \frac{1 - \alpha}{4} \right) \frac{1}{12} \right. \\
 &\quad \left. + M R_m \left( \frac{1 + \alpha}{4} \right) \frac{y}{20} \right\}
 \end{aligned}$$

$$G_1(y) = (y^2 - 1) R_m \left\{ \left( \frac{1-\alpha}{4} \right) \frac{y}{3} + \left( \frac{1+\alpha}{4} \right) \frac{y^2-1}{4} \right\} \quad (5.3.3)$$

We substitute equation (5.3.3) into equations (5.2.17) and (5.2.18) from which the perturbed solution can be obtained. Hence the equations governing the perturbed velocity and magnetic field are

$$\begin{aligned} & (-s_{-1} + R s_0 + R^2 s_1 + \dots) (\phi_{0yy} + R \phi_{1yy} + R^2 \phi_{2yy} + \dots) \\ & + R [ (F_0'' + R F_1'' + \dots) (\phi_0' + R \phi_1' + \dots) \\ & + (F_0' + R F_1' + \dots) (\phi_0'' + R \phi_1'' + \dots) \\ & - (F_0 + R F_1 + R^2 F_2 + \dots) (\phi_0''' + R \phi_1''' + \dots) \\ & - (F_0''' + R F_1''' + R^2 F_2''' + \dots) (\phi_0 + R \phi_1 + \dots) ] \\ & = ( \phi_0^{iv} + R \phi_1^{iv} + R^2 \phi_0^{iv} + \dots ) \\ & + M [ (\lambda_0' + R \lambda_1' + R^2 \lambda_2' + \dots) (R G_1'' + R^2 G_2'' + \dots) \\ & + (\lambda_0'' + R \lambda_1'' + R^2 \lambda_2'' + \dots) (R G_1' + R^2 G_2' + \dots) \\ & - (\lambda_0 + R \lambda_1 + R^2 \lambda_2 + \dots) (R G_1''' + R^2 G_2''' + \dots) \\ & - (G_0 + R G_1 + R^2 G_2 + \dots) (\lambda_0''' + R \lambda_1''' + R^2 \lambda_2''' + \dots) ] \end{aligned} \quad (5.3.4)$$

$$\begin{aligned} & R_m (-s_{-1} + R s_0 + R^2 s_1 + \dots) (\lambda_0 + R \lambda_1 + R^2 \lambda_2 + \dots) \\ & = \lambda_0'' + R \lambda_1'' + R^2 \lambda_2'' + \dots \end{aligned}$$

$$\begin{aligned}
& + R R_m [(\lambda'_0 + R \lambda'_1 + R^2 \lambda'_2 + \dots) (F_0 + R F_1 + \dots) \\
& + (G'_0 + R G'_1 + \dots) (\phi_0 + R \phi_1 + \phi_2 + \dots) \\
& - (\lambda_0 + R \lambda_1 + R^2 \lambda_2 + \dots) (F'_0 + R F'_1 + R^2 F'_2 + \dots) \\
& - (\lambda'''_0 + R \lambda'''_1 + R^2 \lambda'''_2 + \dots) (G_0 + R G_1 + R^2 G_2 + \dots)]
\end{aligned} \tag{5.3.5}$$

We may observe that there exists two families of solutions given by

$$\begin{aligned}
\phi_0(y) &= \cos(n\pi y) - (-1)^n \\
s_{-1} &= n^2 \pi^2 \\
\lambda_0 &= 0 \\
\lambda_1 &= \sin(n\pi \sqrt{R_m} y) \quad \text{if } R_m = \left(\frac{m}{n}\right)^2 \\
&= \cos(n\pi \sqrt{R_m} y) \quad \text{if } R_m = \left(\frac{2m+1}{2n}\right)^2 \\
&= 0 \quad \text{otherwise} \\
s_0 &= -\frac{21}{4} \left(\frac{1+\alpha}{4}\right) \frac{1}{n^2 \pi^2} - 2M \frac{R_m}{R_m - 1} (-1)^{m+n} \\
& \quad \text{if } R_m = \left(\frac{2m+1}{2n}\right)^2 \\
&= -\frac{21}{4} \left(\frac{1+\alpha}{4}\right) \frac{1}{n^2 \pi^2} \quad \text{otherwise}
\end{aligned}$$

$$n, m = 0, \pm 1, \pm 2, \dots \tag{5.3.6}$$

and

$$\begin{aligned}
\phi_0(y) &= y - \frac{\sin(\mu_n y)}{\sin(\mu_n)} \\
s_{-1} &= \mu_n^2 \\
\lambda_0 &= 0 \\
\lambda_1 &= \sin(\mu_n \sqrt{R_m} y) && \text{if } R_m = \left(\frac{m\pi}{\mu_n}\right)^2 \\
&= \cos(\mu_n \sqrt{R_m} y) && \text{if } R_m = \left(\frac{2m+1}{2} \frac{\pi}{\mu_n}\right)^2 \\
&= 0 && \text{otherwise} \\
s_0 &= -\frac{55}{4} \left(\frac{1+\alpha}{4}\right) \frac{1}{\mu_n^2} - 2M \frac{\sqrt{R_m}}{R_m - 1} \frac{(-1)^m}{\mu_n} \\
&= -\frac{55}{4} \left(\frac{1+\alpha}{4}\right) \frac{1}{\mu_n^2} && \text{if } R_m = \left(\frac{2m+1}{2} \frac{\pi}{\mu_n}\right)^2 \\
&&& \text{otherwise} \quad (5.3.7)
\end{aligned}$$

where  $\mu_n$  is defined as the  $n^{\text{th}}$  positive root of the equation  $\tan \mu = \mu$ ,  $n = 1, 2, \dots$ ; The  $\mu_n$  are tabulated in Table 5.1. (Abramowitz and Stegun (1964)). These two families reduce in the case of  $\alpha = 1$ , to symmetric and antisymmetric modes.

We have two additional families of eigensolutions which are entirely due to the effect of magnetic field which are given below.

$$\begin{aligned}
\phi_0(y) &= a_1 y + a_2 \sin\left(\frac{n\pi}{\sqrt{R_m}} y\right) + M \frac{R_m}{1 - R_m} \frac{1}{n^2 \pi^2} \sin(n\pi y) \\
&&& \text{if } R_m \neq 1 \\
&= \frac{M}{2n\pi} [(-1)^n - \cos(n\pi y)] y, && \text{if } R_m = 1
\end{aligned}$$

$$\begin{aligned}
\lambda_0(y) &= \sin(n\pi y) \\
a_1 &= -a_2 \sin\left(\frac{n\pi}{\sqrt{R_m}}\right) \\
a_2 &= M \frac{R_m}{1-R_m} \frac{1}{n\pi} (-1)^n \frac{1}{\sin(n\pi/\sqrt{R_m}) - \sqrt{s_{-1}} \cos(n\pi/\sqrt{R_m})} \\
s_{-1} &= n^2 \pi^2 / R_m \tag{5.3.8}
\end{aligned}$$

Governing equation of  $\lambda_1(y)$  is

$$\begin{aligned}
[\lambda_1'' + R_m s_{-1} \lambda_1] \\
= R_m s_0 \lambda_0 - R_m [\lambda_0' F_0 + G_0' \phi_0 - \lambda_0 F_0' - G_0 \lambda_0'''] \tag{5.3.9}
\end{aligned}$$

The value of  $s_0$  may be obtained from the solvability condition i.e., by multiplying the right hand side of (5.3.9) by  $\lambda_0(y)$ , integrating over the region of flow ( i.e. from  $y = -1$  to  $y = 1$ ) and equating to zero.

Hence  $s_0$  is obtained as

$$s_0 = \frac{1 + \alpha}{4} \frac{1}{n^2 \pi^2} \frac{9}{4} \tag{5.3.10}$$

The other family of eigensolutions is given by

$$\begin{aligned}
\phi_0(y) &= \frac{M}{2} (2n + 1) \frac{\pi}{2} [ (-1)^n y - \sin\left((2n + 1) \frac{\pi}{2} y\right) ] \\
&+ \frac{M}{2} y \cos\left((2n + 1) \frac{\pi}{2} y\right) \quad R_m = 1
\end{aligned}$$

$$\begin{aligned}
&= a_3 y + a_4 \sin(\sqrt{s_{-1}} y) \\
&\quad - M \frac{R_m}{R_m - 1} \frac{1}{\sqrt{s_{-1}} R_m} \sin(\sqrt{s_{-1}} R_m y) \quad R_m \neq 1 \\
a_3 &= -a_4 \cos(\sqrt{s_{-1}}) \sqrt{s_{-1}} \\
a_4 &= M \frac{R_m}{1 - R_m} \frac{(-1)^n}{\sqrt{s_{-1}} R_m [\sin(\sqrt{s_{-1}}) - \sqrt{s_{-1}} \cos(\sqrt{s_{-1}})]} \\
s_{-1} &= (2n+1)^2 \frac{\pi^2}{4} \frac{1}{R_m} \quad n = 0, \pm 1, \pm 2, \dots \\
\lambda_0(y) &= \cos\left((2n+1) \frac{\pi}{2} y\right) \\
s_0 &= \left(\frac{1+\alpha}{4}\right) \frac{9}{(2n+1)^2 \pi^2} \tag{5.3.11}
\end{aligned}$$

We observe that the stability parameter depends only on the parameter combination  $(1 + \alpha)$ . A similar pattern was found by Cox (1991) in his analysis of channel flow with unequal suction at the two walls. It is readily seen that when  $\alpha = 1$  and  $M = 0$  the previous result of Watson et al (1990) is recovered. Again, we may retrace the solutions obtained by Watson *et al* (1990) for the limiting case of  $M \rightarrow 0$ .

Table 5.1

Roots  $\mu_n$  of  $\tan \mu_n = \mu_n$ 

$\mu_n$	Value of $\mu_n$
$\mu_1$	2.02876
$\mu_2$	4.91318
$\mu_3$	7.97867
$\mu_4$	11.08554
$\mu_5$	14.20744
$\mu_6$	17.33638
$\mu_7$	20.46917
$\mu_8$	23.60428
$\mu_9$	26.74092

#### 5.4. Analysis for large R

Watson *et al* (1990, 1991) investigated the structure of the asymptotic solutions for large positive R in the case of  $\alpha = 1$  and in the absence of magnetic field. It was found that for the symmetric flow, there were boundary layers with thickness of order of magnitude  $R^{-1/2}$  at the two walls and a weak inviscid core driven by the boundary layer flows.

The assumed structures of the asymptotic solutions below are based on the literature (Terrill (1964) and Brady and Acrivos (1981), Watson *et al* (1991)) and trial and error.



We assume that the moving walls drive an inviscid core at  $y = \pm 1$ . Also we shall assume that the first order term in the inviscid core is weak and  $o(1)$  for large  $R$ .

We assume that the boundary layer solutions at the two walls are found to be of the form

$$\begin{aligned}
 F(y,R) &= R^{-1/2} \phi^+(\eta, R) \\
 G(y,R) &= \psi^+(\eta, R) \\
 F(y,R) &= R^{-1/2} \phi^-(\zeta, R) \\
 G(y,R) &= \psi^-(\zeta, R)
 \end{aligned} \tag{5.4.1}$$

where  $\eta$  and  $\zeta$  are the stretch variables in the boundary layer and are given as

$$\begin{aligned}
 \eta &= R^{1/2} (1 - y) \\
 \zeta &= R^{1/2} (1 + y)
 \end{aligned} \tag{5.4.2}$$

We expand  $\phi^+$ ,  $\phi^-$ ,  $\psi^+$ ,  $\psi^-$  in the powers of  $R^{-1/2}$  as

$$\begin{aligned}
 \phi^+(\eta,R) &= \phi_0^+(\eta) + R^{-1/2} \phi_1^+(\eta) + \dots \\
 \phi^-(\zeta,R) &= \phi_0^-(\zeta) + R^{-1/2} \phi_1^-(\zeta) + \dots \\
 \psi^+(\eta,R) &= \psi_0^+(\eta) + R^{-1/2} \psi_1^+(\eta) + \dots \\
 \psi^-(\zeta,R) &= \psi_0^-(\zeta) + R^{-1/2} \psi_1^-(\zeta) + \dots
 \end{aligned}$$

as  $R \rightarrow \infty$  for fixed  $\eta, \zeta$  (5.4.3)

The boundary conditions (5.2.16) will become

$$\begin{aligned}\phi^+(\eta, R) &= 0 ; \frac{\partial \phi^+}{\partial \eta} = -1 ; \quad \psi^+(\eta, R) = 1 \quad \text{at } \eta = 0 \\ \phi^-(\zeta, R) &= 0 ; \frac{\partial \phi^-}{\partial \zeta} = \alpha ; \quad \psi^-(\zeta, R) = 1 \quad \text{at } \zeta = 0\end{aligned}$$

Hence the conditions that are to be satisfied by  $\phi_n$  and  $\psi_n$  are

$$\begin{aligned}\phi_0^+(0) &= 0 ; \phi_0^{+'}(0) = -1 ; \quad \psi_0^+(0) = 1 ; \\ \phi_n^+(0) &= 0 ; \phi_n^{+'}(0) = 0 ; \quad \psi_n^+(0) = 0 ; \quad n \geq 1 \\ \phi_0^-(0) &= 0 ; \phi_0^{-'}(0) = \alpha ; \quad \psi_0^-(0) = 1 ; \\ \phi_n^-(0) &= 0 ; \phi_n^{-'}(0) = 0 ; \quad \psi_n^-(0) = 0 ; \quad n \geq 1\end{aligned}\tag{5.4.4}$$

Substituting equation (5.4.3) in (5.2.15), we obtain the equations that are satisfied by  $\phi_n$  and  $\psi_n$  as follows :

$$\begin{aligned}\frac{\partial^2 \psi_0^+(\eta)}{\partial \eta^2} &= 0 \\ \frac{\partial^2 \psi_1^+(\eta)}{\partial \eta^2} &= 0\end{aligned}\tag{5.4.5}$$

$$\begin{aligned}\frac{\partial^4 \phi_0^+(\eta)}{\partial \eta^4} - \phi_0^+ \frac{\partial^3 \phi_0^+(\eta)}{\partial \eta^3} + \frac{\partial \phi_0^+(\eta)}{\partial \eta} \frac{\partial^2 \phi_0^+(\eta)}{\partial \eta^2} \\ + S^2 \frac{\partial^3 \psi_2^+(\eta)}{\partial \eta^3} &= 0\end{aligned}\tag{5.4.6}$$

$$\frac{\partial^2 \psi_2^+(\eta)}{\partial \eta^2} + R_m \frac{\partial \phi_0^+(\eta)}{\partial \eta} = 0\tag{5.4.7}$$

$$\begin{aligned}\frac{\partial^4 \phi_1^+(\eta)}{\partial \eta^4} - \phi_0^+ \frac{\partial^3 \phi_1^+(\eta)}{\partial \eta^3} + \frac{\partial \phi_0^+(\eta)}{\partial \eta} \frac{\partial^2 \phi_1^+(\eta)}{\partial \eta^2} \\ - \phi_1^+ \frac{\partial^3 \phi_0^+(\eta)}{\partial \eta^3} + \frac{\partial \phi_1^+(\eta)}{\partial \eta} \frac{\partial^2 \phi_0^+(\eta)}{\partial \eta^2}\end{aligned}$$

$$+ S^2 \frac{\partial^3 \psi_3^+(\eta)}{\partial \eta^3} = 0 \quad (5.4.8)$$

$$\frac{\partial^2 \psi_3^+(\eta)}{\partial \eta^2} + R_m \frac{\partial \phi_1^+(\eta)}{\partial \eta} = 0 \quad (5.4.9)$$

Equations (5.4.5) - (5.4.9) together with the boundary conditions (5.4.4) yield the following solutions

$$\psi_0^+(\eta) = 1$$

$$\psi_1^+(\eta) = 0$$

$$\phi_0^+(\eta) = \frac{1}{\lambda} - \frac{1}{\lambda} \exp \{ \lambda \eta \}$$

$$\psi_2^+(\eta) = \frac{R_m}{\lambda^2} [ \exp \{ \lambda \eta \} - 1 ]$$

$$\phi_1^+(\eta) = e^{\lambda \eta} \int_0^{\eta} F_2(y_1) \int_0^{y_1} \exp \left[ \int_0^{y_2} F_3(y_3) dy_3 \right] dy_2 dy_1$$

where

$$F_3(\eta) = - \frac{1}{\lambda F_2(\eta)} \left\{ \frac{3 + 5 S^2 R_m}{1 + 2 S^2 R_m} + \frac{e^{\lambda \eta}}{1 + 2 S^2 R_m} + S^2 R_m e^{-\lambda \eta} \right\}$$

$$F_2(\eta) = \frac{1}{1 + 2 S^2 R_m} + \exp [ - \lambda \eta ]$$

$$\lambda = - \sqrt{1 + S^2 R_m} \quad (5.4.10)$$

In a similar manner, the solution for  $\phi^-$  and  $\psi^-$  are obtained as

$$\psi_0^-(\zeta) = 1$$

$$\psi_1^-(\zeta) = 0$$

$$\phi_0^-(\zeta) = \frac{\alpha}{\lambda} [-1 + \exp \{\lambda \zeta\}]$$

$$\psi_2^-(\zeta) = \frac{\alpha R_m}{\lambda^2} [\exp \{\lambda \zeta\} - 1]$$

$$\phi_1^-(\zeta) = e^{\lambda \zeta} \int_0^{\zeta} F_2(y_1) \int_0^{y_1} \exp \left[ \int_0^{y_2} F_3(y_3) dy_3 \right] dy_2 dy_1$$

where

$$F_3(\zeta) = -\frac{1}{\lambda F_2(\zeta)} \left\{ \frac{(3\alpha + 5 S^2 R_m) \alpha}{\alpha + 2 S^2 R_m} + \alpha^2 \frac{e^{\lambda \zeta}}{\alpha + 2 S^2 R_m} + S^2 R_m e^{-\lambda \zeta} \right\}$$

$$F_2(\zeta) = \frac{\alpha}{\alpha + 2 S^2 R_m} + \exp [-\lambda \zeta]$$

$$\lambda = -\sqrt{\alpha + S^2 R_m} \quad (5.4.11)$$

We assume that there is an outer solution of the form

$$F(y, R) = R^{-1/2} \Phi(y, R)$$

$$G(y, R) = R^{-1/2} \Psi(y, R)$$

where

$$\Phi(y, R) = \Phi_0(y) + R^{-1/2} \Phi_1(y) + \dots$$

$$\Psi(y, R) = \Psi_0(y) + R^{-1/2} \Psi_1(y) + \dots$$

$$\text{as } R \rightarrow \infty \text{ for fixed } y \neq \pm 1 \quad (5.4.12)$$

Hence we get

$$\begin{aligned}
 \Phi_0(y) &= a_3 + a_4 y \\
 \Psi_0(y) &= a_1 + a_2 y \\
 \Psi_1(y) &= a_5 (1 - y^2)
 \end{aligned} \tag{5.4.13}$$

To determine  $\Phi$  and  $\Psi$  completely, we assume that the inner and outer solutions match at the edge of the boundary layer i.e.,

$$\begin{aligned}
 \lim_{y \rightarrow 1} \Phi(y) &= \lim_{\eta \rightarrow \infty} \phi_1^+(\eta) \\
 \lim_{y \rightarrow -1} \Phi(y) &= \lim_{\zeta \rightarrow \infty} \phi_1^-(\zeta)
 \end{aligned} \tag{5.4.14}$$

Hence the solutions for  $\Phi$  and  $\Psi$  are as given below

$$\begin{aligned}
 \Psi_0(y) &= 1 \\
 \Phi_0(y) &= \frac{1}{2} \left[ -\frac{1}{\sqrt{1+S^2R_m}} + \frac{\alpha}{\sqrt{\alpha+S^2R_m}} \right] \\
 &\quad - \frac{1}{2} \left[ \frac{1}{\sqrt{1+S^2R_m}} + \frac{\alpha}{\sqrt{\alpha+S^2R_m}} \right] y \\
 \Psi_1(y) &= \frac{R_m}{4} \left[ \frac{1}{\sqrt{1+S^2R_m}} + \frac{\alpha}{\sqrt{\alpha+S^2R_m}} \right] (1 - y^2) \\
 \Phi_1(y) &= a_6 + 2 \frac{a_7}{R_m} y \\
 &\quad + \frac{1}{2} \frac{R_m}{4} \left[ \frac{1}{\sqrt{1+S^2R_m}} + \frac{\alpha}{\sqrt{\alpha+S^2R_m}} \right]^2 y
 \end{aligned}$$

$$- \frac{1}{4} a_6 \frac{y^2}{2} + \frac{R_m}{4} \left[ \frac{1}{\sqrt{1+S^2R_m}} + \frac{\alpha}{\sqrt{\alpha+S^2R_m}} \right]^2 \frac{y^3}{3}$$

$$\begin{aligned} \Psi_2(y) = & a_5 + a_6 y + a_7 y^2 \\ & + \frac{R_m^2}{4} \left[ \frac{1}{\sqrt{1+S^2R_m}} + \frac{\alpha}{\sqrt{\alpha+S^2R_m}} \right]^2 \frac{y^4}{24} \end{aligned} \quad (5.4.15)$$

where

$$\begin{aligned} a_5 = & -R_m \left[ \frac{1}{1+S^2R_m} + \frac{\alpha}{\alpha+S^2R_m} \right] \\ & - \frac{R_m^2}{96} \left[ \frac{1}{\sqrt{1+S^2R_m}} + \frac{\alpha}{\sqrt{\alpha+S^2R_m}} \right]^2 - a_7 \end{aligned}$$

$$a_6 = R_m \left[ -\frac{1}{1+S^2R_m} + \frac{\alpha}{\alpha+S^2R_m} \right]$$

$$a_7 = \frac{R_m}{2} \left\{ A_1 - A_2 - \frac{5}{24} R_m \left[ \frac{1}{\sqrt{1+S^2R_m}} + \frac{\alpha}{\sqrt{\alpha+S^2R_m}} \right]^2 \right\}$$

$$a_8 = A_1 + A_2 + \frac{R_m}{8} \left[ \frac{1}{1+S^2R_m} + \frac{\alpha}{\alpha+S^2R_m} \right]$$

$$A_1 = \phi_1^+(\infty)$$

$$A_2 = \phi_1^-(\infty)$$

The solution requires  $\alpha > 0$  and  $\alpha^{1/2}R \geq 1$ . For  $R_m = 0 = S$  the above solution reduces to the solution found by Watson *et al* (1991) who used the fact that the integral

$$I = \int_0^1 [e^{-s}((1+s)^{-1} + (1+s)^{-2}) + s^{-1}] ds$$

$$= 1 - \frac{1}{2} e^{-1} + \gamma + E_1(1) \quad (5.4.16)$$

to determine  $A_1$  and  $A_2$  where  $\gamma$  is Eulers' constant and  $E_1(x)$  is the exponential integral. We find  $I = 1.6127$ .

### 5.5. Numerical results

In the previous section, effort has been devoted to the development of asymptotic techniques incorporating the magnetic terms to obtain acceptable approximations for the steady and perturbed state velocity and magnetic field. For the present, we confine our results related to various values of  $\alpha$  for the basic flow and present numerical results for the eigenvalues as functions of the non-dimensional parameter  $R$ .

Our understanding of the transition from laminar to turbulent motion is still far from complete. In the past decade there has been much progress towards an understanding of the transition from laminar to turbulent flow. It has become clear that there are various possible routes to this transition involving a sequence of bifurcations. Hence the attention of research in hydrodynamic stability theory is focussed on a quantitative treatment of special problems which can be solved and compared with experiments.

The stability of the basic flow depends on the behaviour of solutions after a long time rather than on their initial behaviour. The increasing complexity of fluid motions which is observed as the viscosity is decreased is a manifestation of the successive loss of stability of flows

15701

of less complicated structure to those with a more complicated structure. When the data is steady and the viscosity is high, all solutions are attracted to the steady basic flow. The simplest non-trivial steady flows arise in two-dimensional hydrodynamics. The structures of zonal winds in the atmospheres of the Earth, Jupiter and Saturn have been related to such flows.

It is conventional and frequently convenient to use a Reynolds number rather than the viscosity as the characterizing parameter for stability analysis. Hence skin friction associated with the steady state velocity is presented as a function of Reynolds number in figures (5.1) - (5.3). Various branches of steady solutions are found, with hysteresis, turning points and pitchfork bifurcations and are shown in figures (5.1) - (5.3).

We describe the case when  $R > 0$ . In figure (5.1) we have reproduced the asymmetric solutions obtained by Watson *et al* (1990) which arise from a pitchfork bifurcation at  $R = R_1$ .

The effect of magnetic field has been shown in the subsequent figures(5.2) and (5.3). From these figures, we can observe that the critical Rayleigh number occurs at an earlier stage for increasing magnetic parameter.

When the boundary conditions are symmetric, a detailed study of the basic flow, and of the eigenvalue problem was made by Watson *et*



al (1990). The purpose of the present section is to present numerical results for various values of  $\alpha$ .

We have computed the steady skin friction  $F''(1)$  and  $F''(-1)$  at both the walls and depicted the values in figures (5.4) - (5.9).

Brady and Acrivos (1981) has studied the basic flow governed by equation (5.2.2) in the absence of magnetic field subject to symmetric boundary conditions,  $\alpha = 1$ . For a given large  $R$ , they have found that the multiple solutions have the same skin friction  $F''(1, R)$ . In our analysis, restricted to the case of asymptotically small  $R$ , the magnitude of the skin friction is enhanced by the increasing value of  $M$  (Figures (5.4) and (5.7))

In figures (5.5), (5.6), (5.8) and (5.9) we have plotted the skin friction at the accelerating walls  $y=-1$  and  $y=1$  as a function of Reynolds number  $R$  for fixed  $M$  ( $= 0.0, 10.0$ ). It can be observed from the figures, that skin friction increases as  $\alpha$  increases.

We next concentrate on the effects of various parameters such as  $\alpha$ ,  $M$ ,  $R$  on the eigenvalues of the problem. As was mentioned in the previous problem we have four families of waves out of which two families of waves exist entirely due to the magnetic field.

The eigenvalue (mode a) related to the solution

$$\begin{aligned}\phi_0(y) &= a_1 y + a_2 \sin\left(\frac{n\pi}{\sqrt{R_m}}\right) + M \frac{R_m}{1-R_m} \frac{1}{n^2 \pi^2} \sin(n\pi y) \\ &\quad \text{if } R_m \neq 1 \\ &= \frac{M}{2n\pi} [(-1)^n - \cos(n\pi y)] y \quad \text{if } R_m = 1\end{aligned}$$

is given by

$$s = -\frac{n^2 \pi^2}{R R_m} + \left(\frac{1+\alpha}{4}\right) \frac{1}{n^2 \pi^2} \frac{9}{4} \quad n = \pm 1, \pm 2, \dots$$

In this case it is obvious that the frequency of the disturbances depends on the inverse of the Reynolds number and magnetic Reynolds number. It is clearly seen in figure (5.10) for, for very small values of  $R$ , we observe a boom in the value of  $s$ , then a steep depression as  $R$  increases. For moderate values of  $R$ ,  $s$  decreases gradually to attain a constant value. In the same way, increasing  $R_m$ , causes a decrease in the growth rate of the perturbation. Here the value of  $n$  is taken to be unity. It should be noted that, it is possible to have stable waves, by selecting suitably large values for  $n$ . Also, from figure (5.11), it can be understood that increasing  $\alpha$ , increases the magnitude of  $s$ , and thereby increasing the instability of the system.

Now, we discuss the second family of waves (mode b) that exist due to the presence of magnetic field. The eigenvalue is given by the expression

$$s = -(2n+1)^2 \frac{\pi^2}{4} \frac{1}{R R_m} + \left(\frac{1+\alpha}{4}\right) \frac{9}{(2n+1)^2 \pi^2} \quad n = \pm 1, \pm 2, \dots$$

As in mode (a), here also the frequency is a function of  $R^{-1}$  and  $R_m^{-1}$ . The dependence of  $s$  on  $R$ ,  $R_m$  and  $\alpha$  is shown in figures (5.12) and (5.13). Increasing  $R$  and  $R_m$  decreases the value of  $s$  and increasing  $\alpha$  increases the value of  $s$ .

We find two more families of waves (mode c and d ) which, in the absence of magnetic field, reduce to those relations derived by Watson *et al* (1991). These two families of solutions reduce in the case  $\alpha = 1$  to antisymmetric and symmetric modes. In both the families of waves, we note that the presence of magnetic field affects the growth rate only for specific values of  $R_m$  and for the remaining values of  $R_m$ ,  $s$  is left unaffected. Also the effect of  $M$  on  $s$  is not uniform as when  $R_m = 1/4$  increase in  $M$  increases the magnitude of  $s$  (Figure (5.14)) and when  $R_m = (21/20)^2$ , magnitude of  $s$  decreases as  $M$  increases (Figure (5.15)). This can be more clearly understood from figures (5.16) and (5.17) where the value of growth rate is expressed as a function of  $R$  for various values of  $R_m$  and  $M$ .

The qualitative behaviour of the families of waves (c) and (d) are similar which can be understood by comparing the figures (5.19) - (5.22) with figures (5.15) - (5.18). In both the cases, it may be observed that for very small values of  $R$ ,  $s$  is increasing rapidly to attain a maximum and then becomes constant for increasing  $R$ . This behaviour can also be predicted from the expressions derived for  $s$  in the previous section.

## 5.5. Conclusion

We have considered a two-dimensional flow of an incompressible, electrically conducting, viscous fluid in a channel confined between the walls at  $y = 1$  and  $y = -1$ , the flow is driven by accelerating walls. To reduce the complexity of the problem, we have made use of Hiemenz similarity form. A small sinusoidal disturbance has been imposed on the stationary state variables and normal mode approach to linear stability has been used. We have made the simplifying assumption of small Reynolds number to solve the governing equations of the problem. For small Reynolds number, asymptotic series solutions of steady state and perturbed state velocities are obtained. The results so obtained are studied numerically.

In steady state solution, obtained numerically we observe pitchfork bifurcations which occur at smaller values of Reynolds number for increasing magnetic parameter.

When a magnetic field is present, we have four families of eigenvalues. Skin friction increases due to the increase in the magnetic interaction number. All the waves have high frequency for very small  $R$  and the growth rate becomes constant as  $R$  increases. Increasing  $R_m$  decreases the value of  $s$ .

The structure of the asymptotic solutions for large positive  $R$  has also been investigated. It was found that there were boundary layers with thickness of order of magnitude  $R^{-1/2}$  at the two walls and weak inviscid core driven by the boundary layer flows.

These asymptotic results are useful to start iterations of numerical approximations to the steady flows and their stability characteristics.

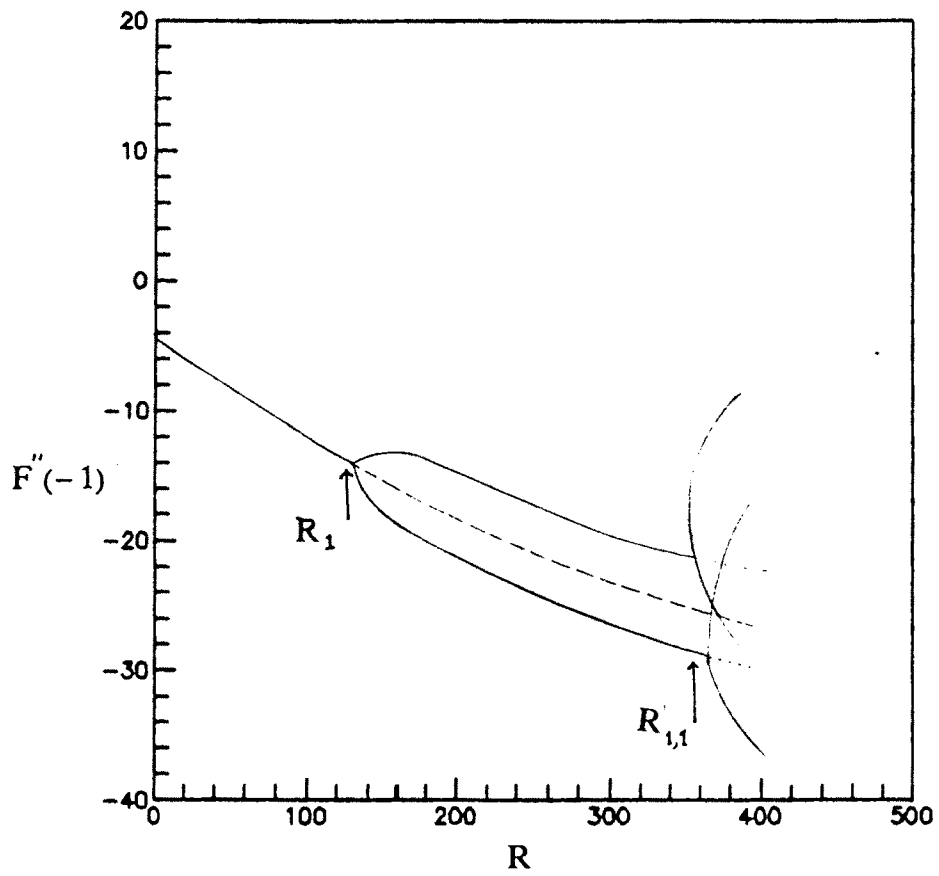


Fig. 5.1. Skin friction  $F''(-1)$  as a function of  $R$   
( $S = 0.0$ )

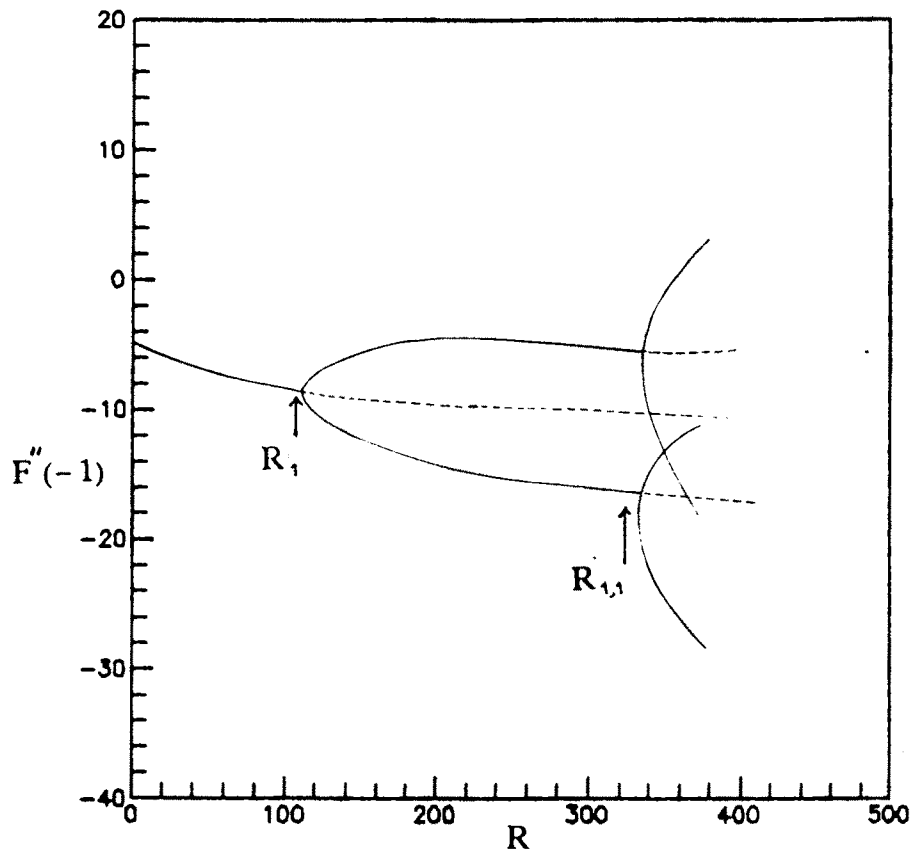


Fig. 5.2. Skin friction  $F''(-1)$  as a function of  $R$   
( $S = 0.1$ )

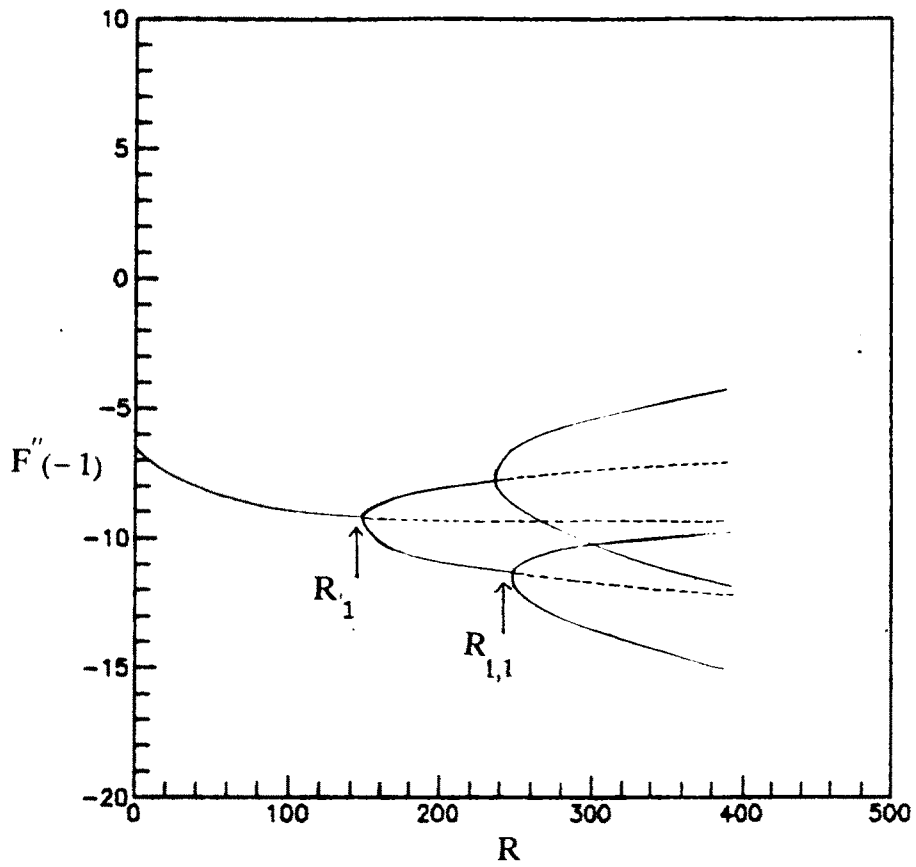


Fig. 5.3. Skin friction  $F''(-1)$  as a function of  $R$   
( $S = 1.0$ )

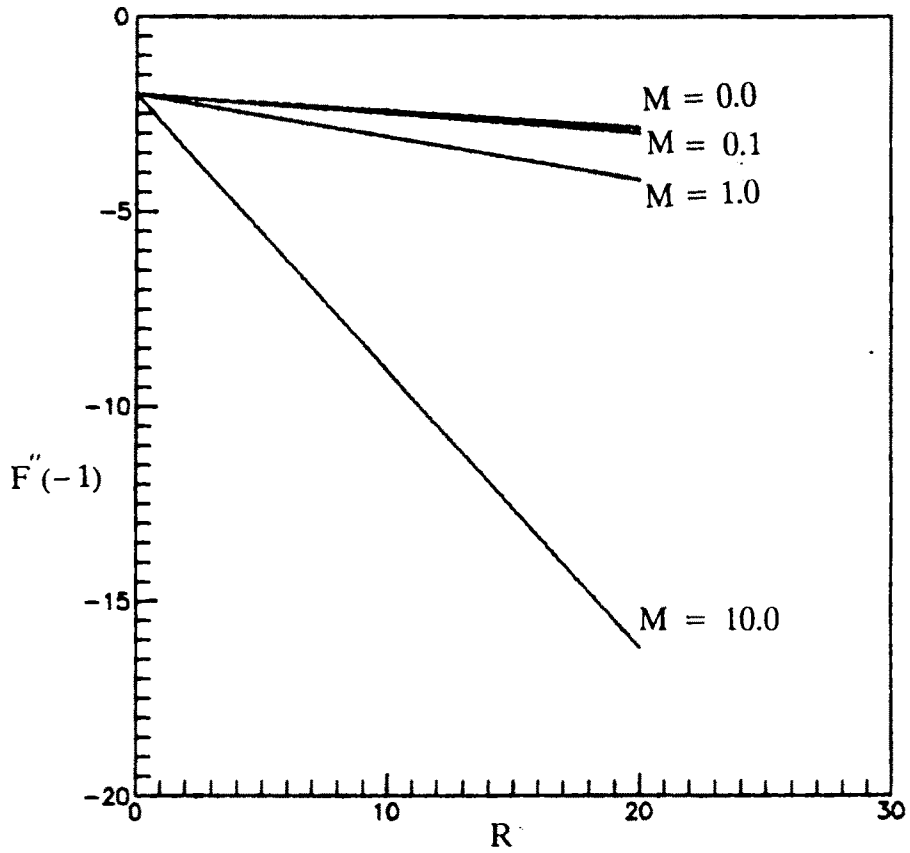


Fig. 5.4. Skin friction  $F''(-1)$  at  $y = -1$  as a function of  $R$  ( $\alpha = 0.5$ )



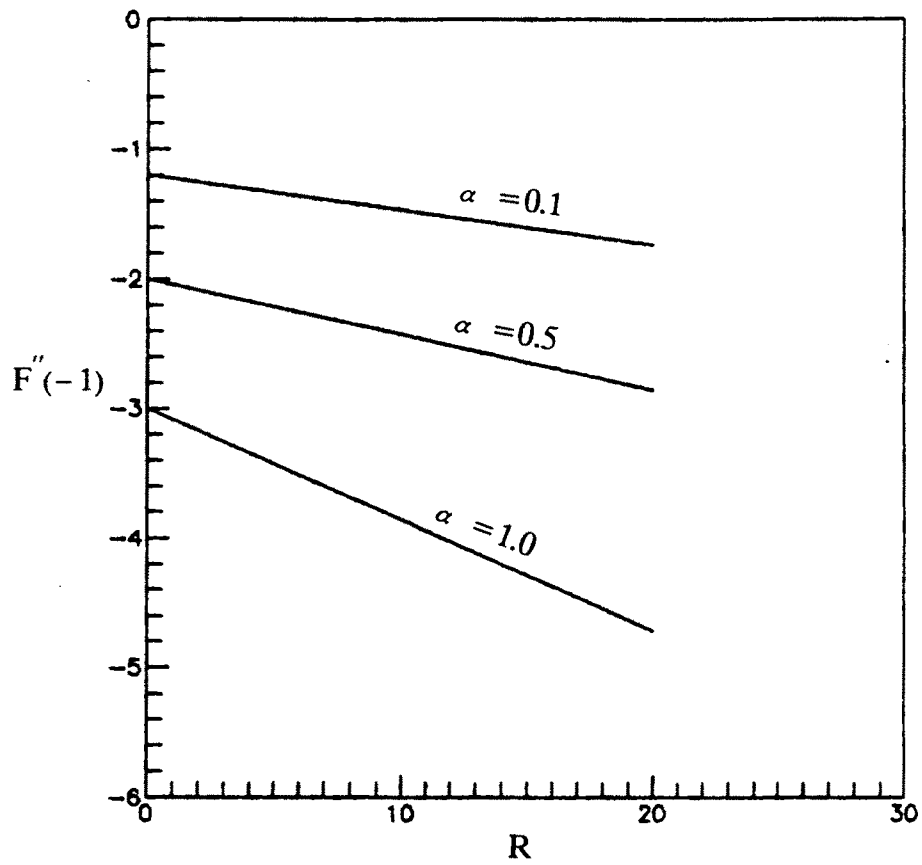


Fig. 5.5. Skin friction  $F''(-1)$  at  $y = -1$  for various values of  $\alpha$  ( $M = 0.0$ )

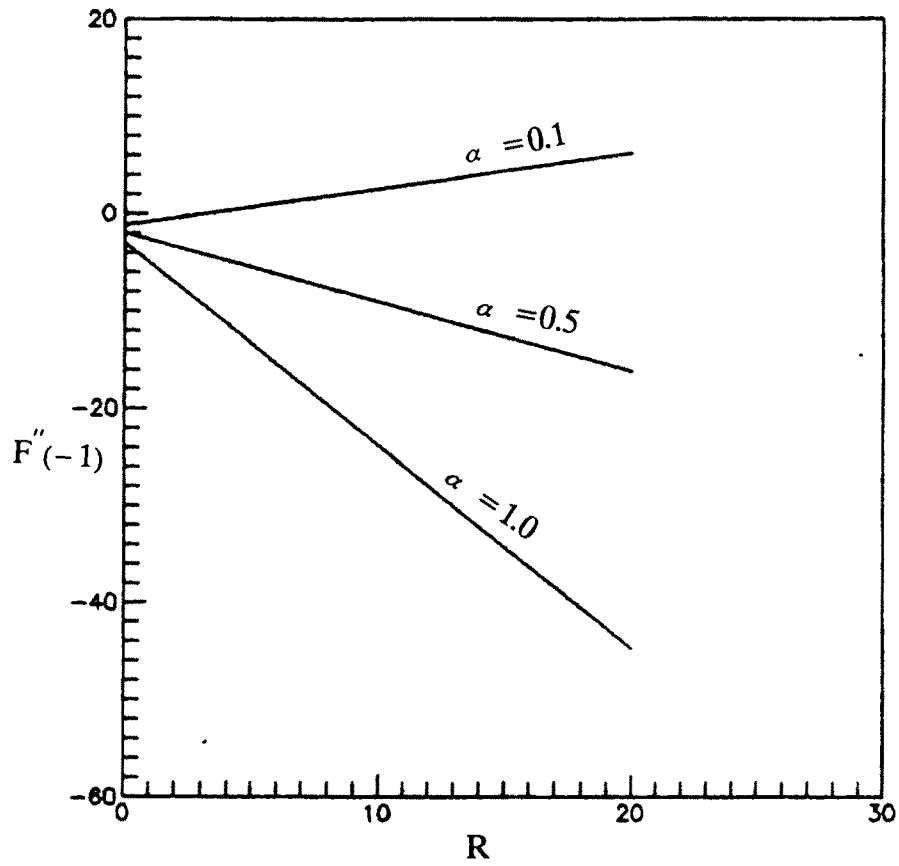


Fig. 5.6. Skin friction  $F''(-1)$  at  $y = -1$  for various values of  $\alpha$  ( $M = 10.0$ ).

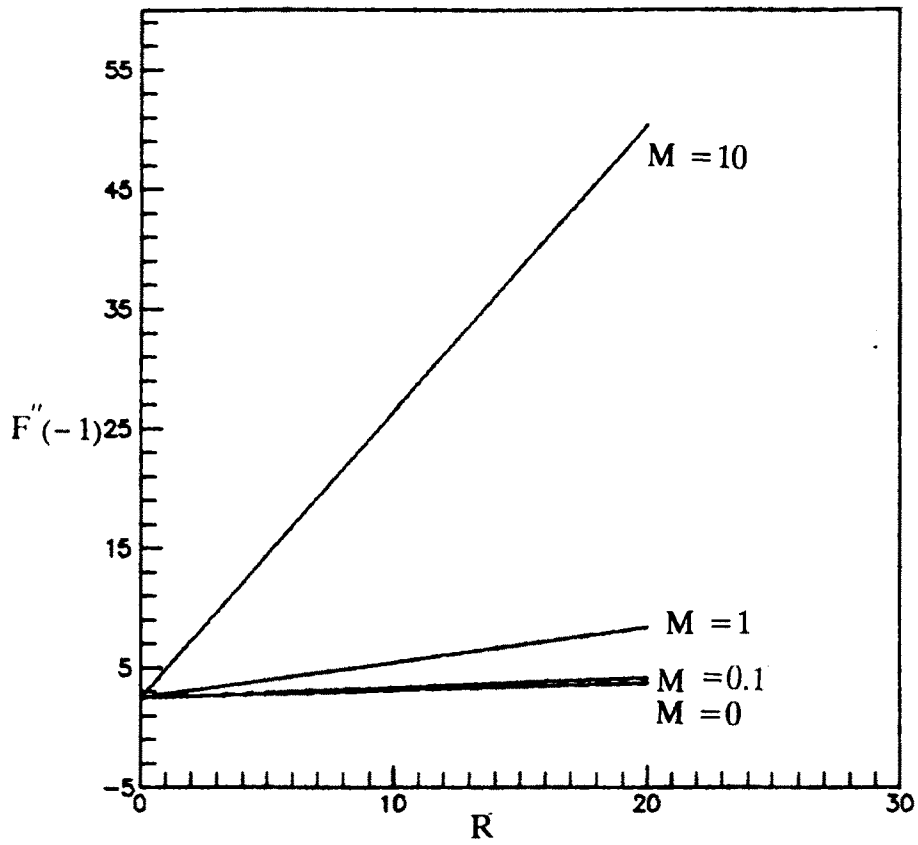


Fig. 5.7. Skin friction  $F''(-1)$  at  $y = -1$  for  $\alpha = 0.5$  as a function of  $R$

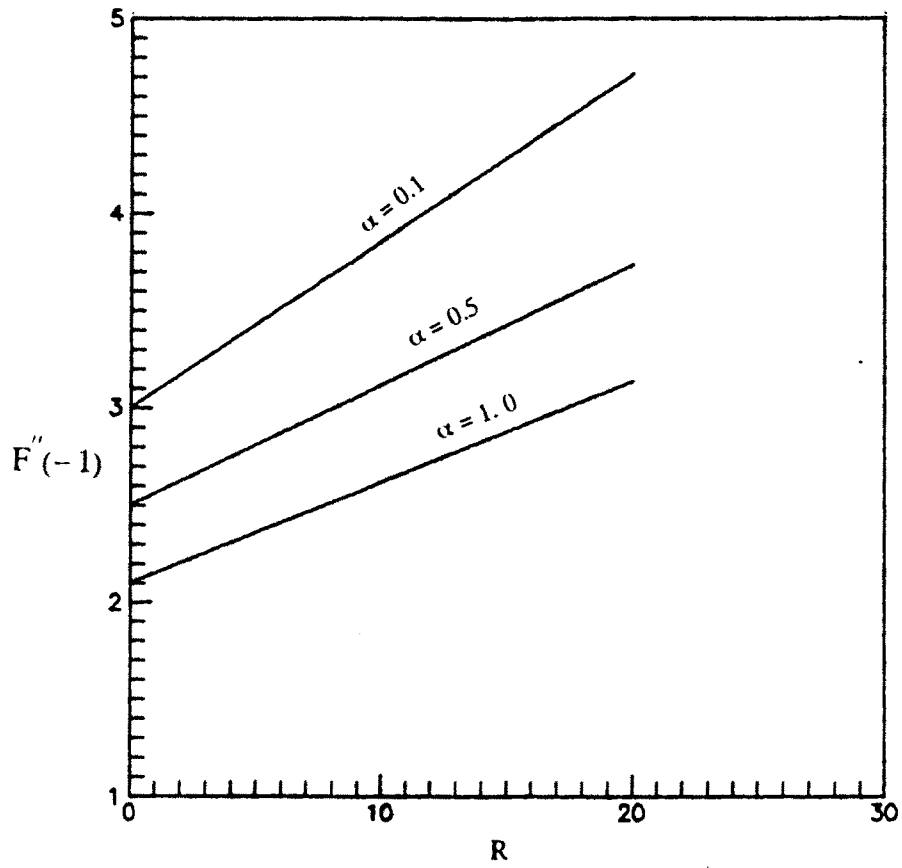


Fig. 5.8. Variation of  $F''(1)$  as a function of  $R$   
( $M = 0.0$ )

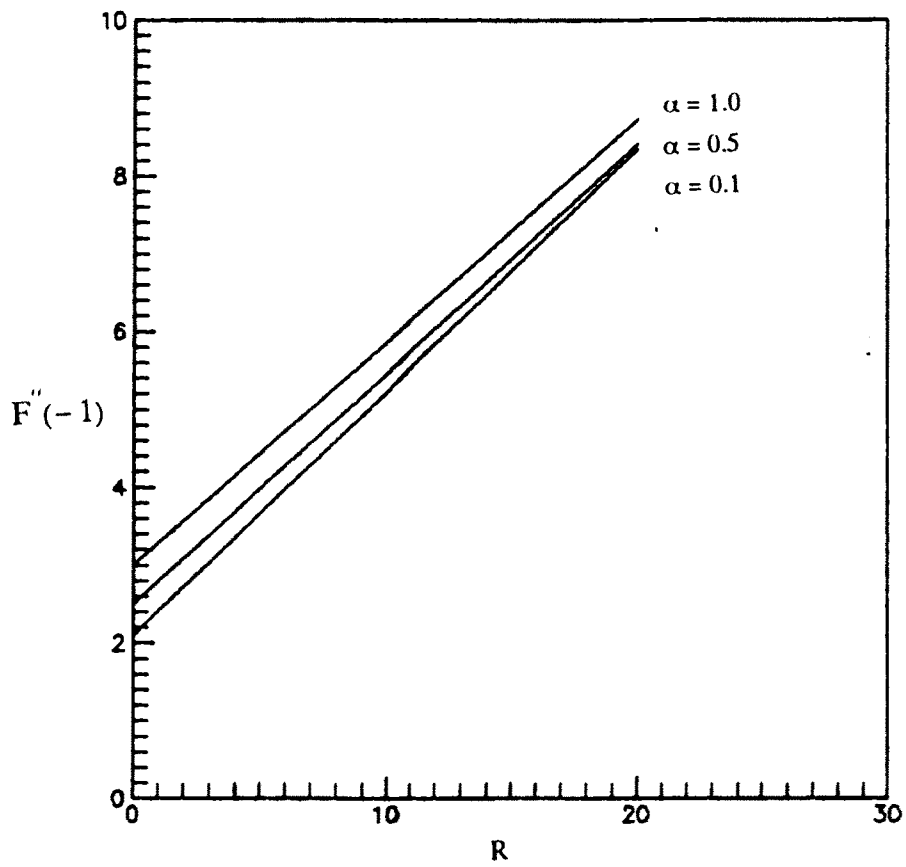


Fig. 5.9. Variation of  $F''(1)$  as a function of  $R$   
( $M = 1.0$ )

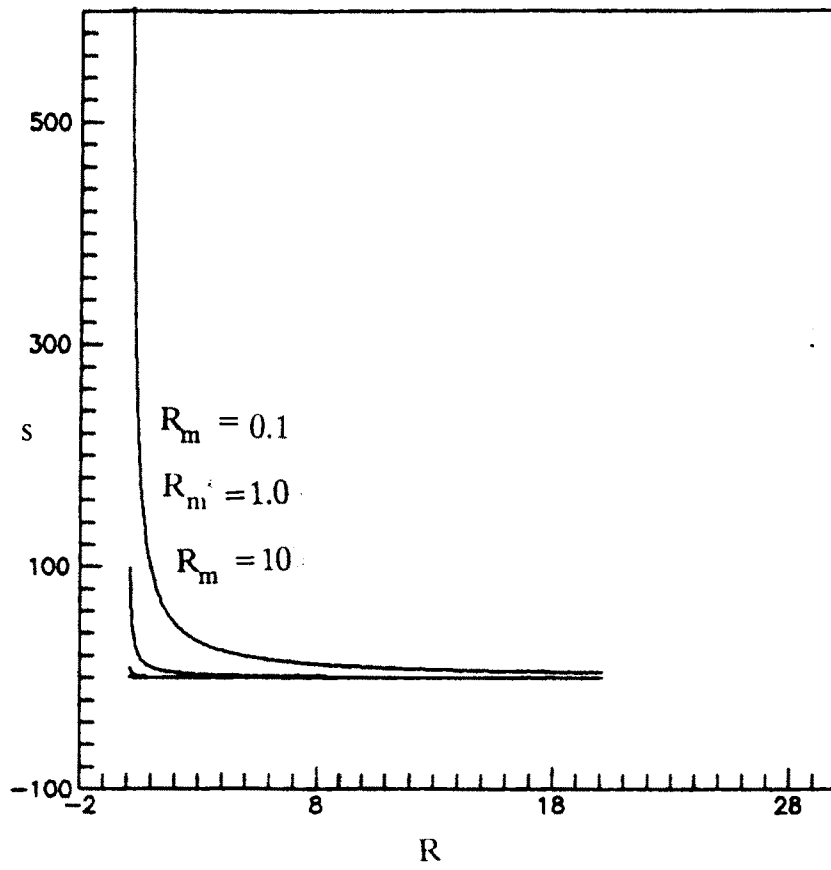


Fig. 5.10. Growth rate  $s$  as a function of  $R$  for different values of  $R_m$  (Mode a)

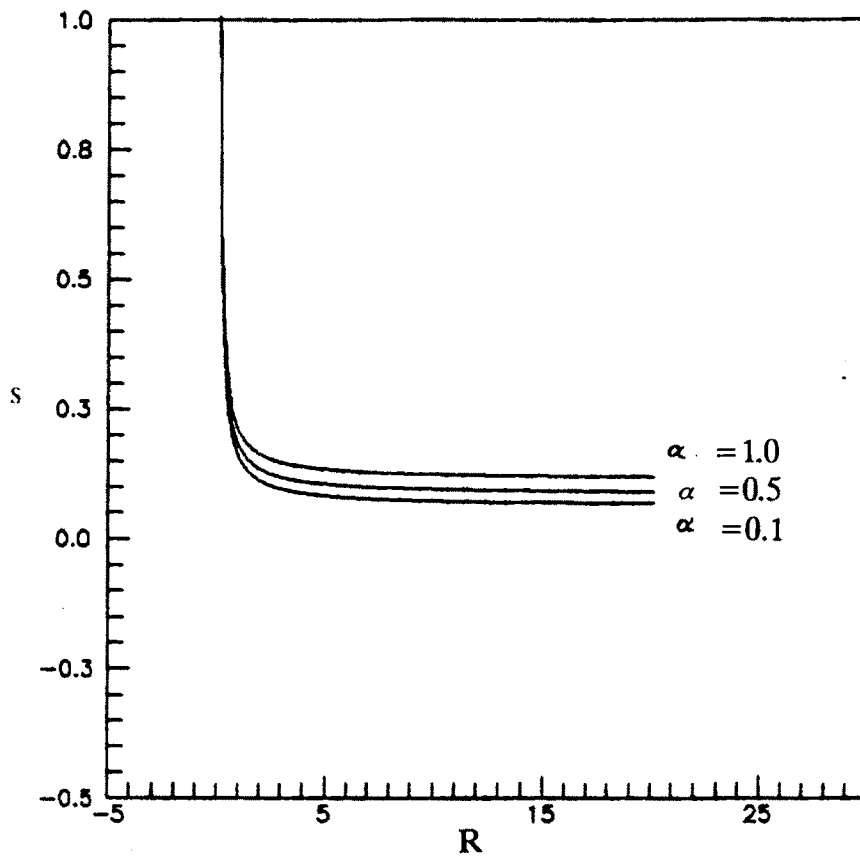


Fig. 5.11. Growth rate  $s$  against  $R$  for different values of  $\alpha$  (Mode a)

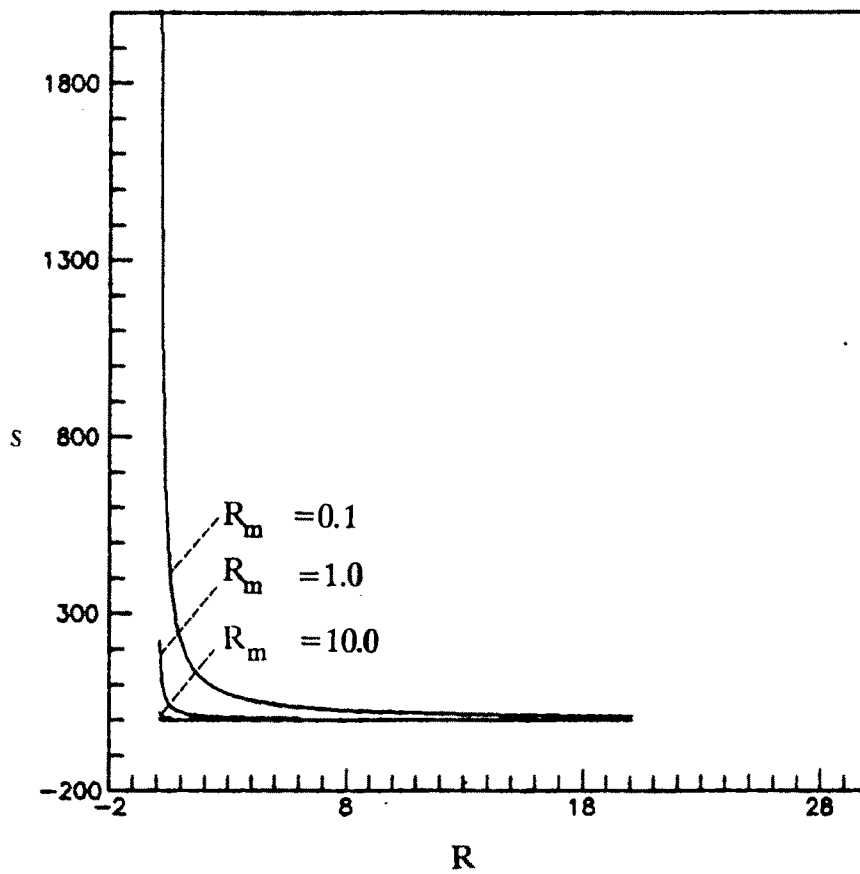


Fig. 5.12. Growth rate  $s$  against  $R$  for different values of  $R_m$  (Mode b)



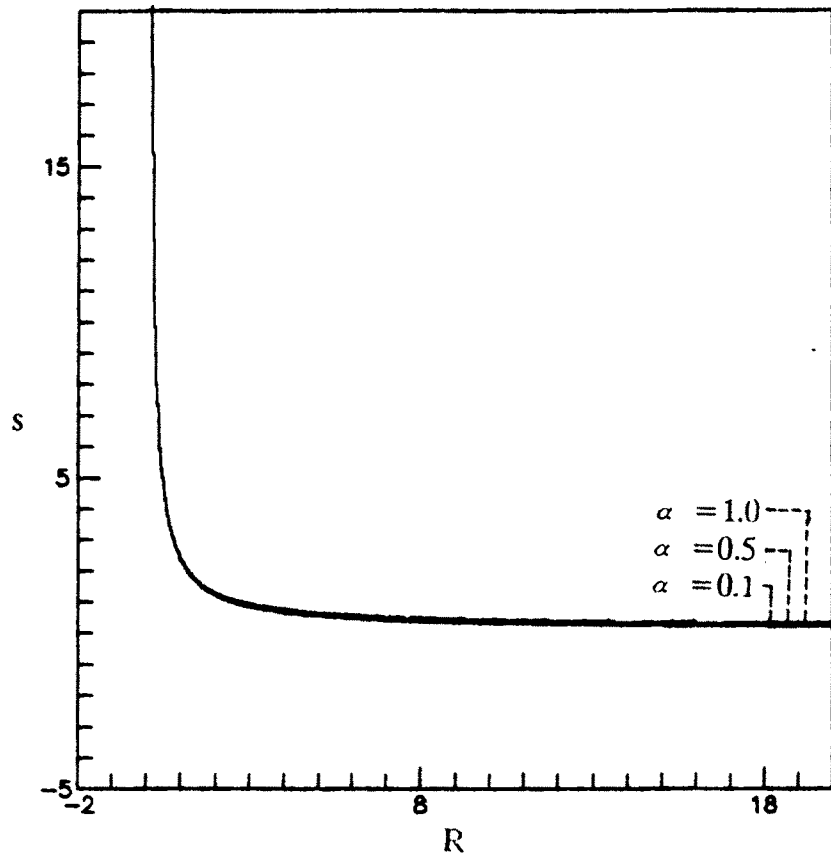


Fig. 5.13. Growth rate  $s$  as function of  $R$  for  $R_m = 10.0$  (Mode b)

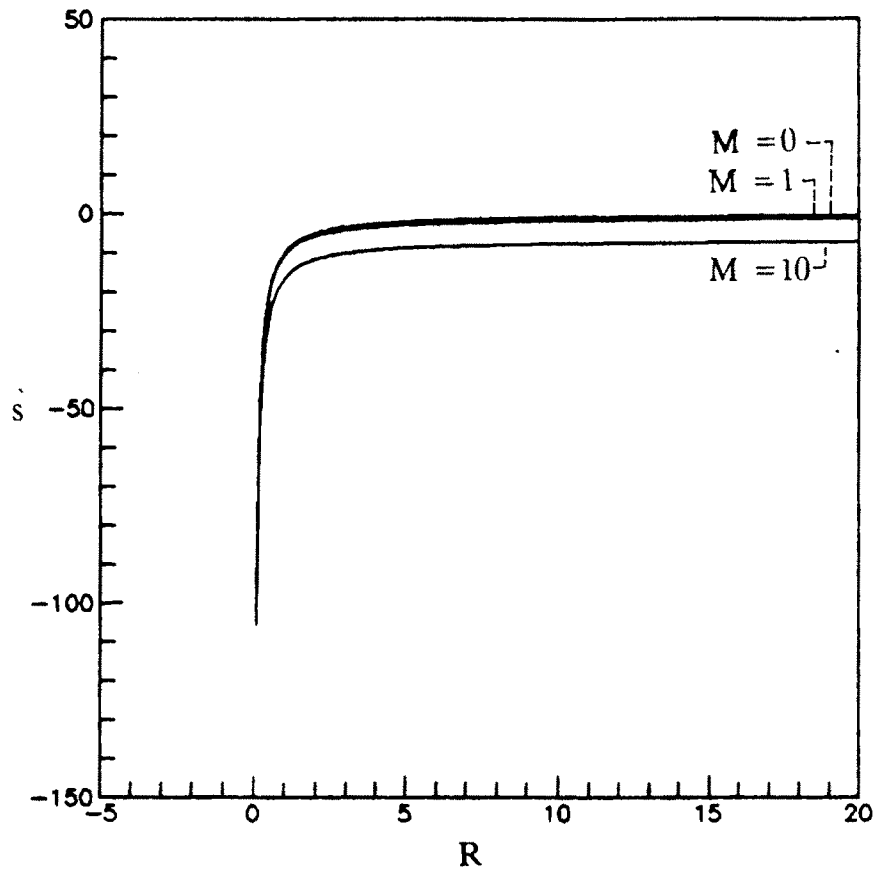


Fig. 5.14. Eigenvalues as functions of  $R$  for  $\alpha = 0.1$   
 $m = 0.0$  (Mode c)

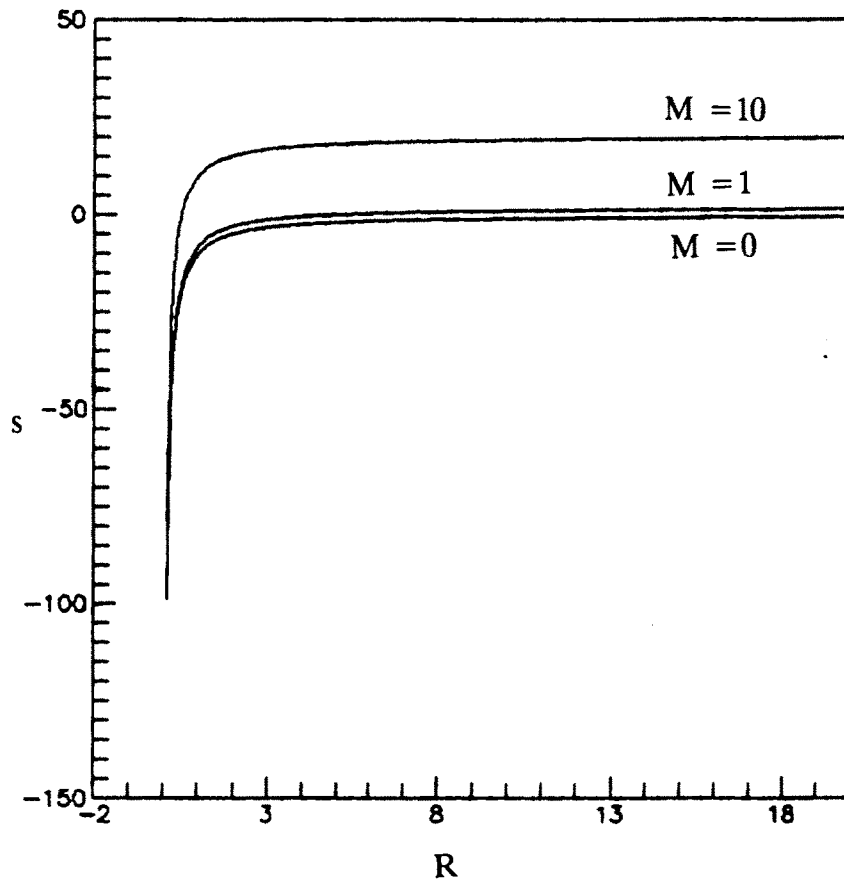


Fig. 5.15. Dependence of  $s$  on  $R$  for  $\alpha = 0.1$   
 $m = 10.0$  (Mode c)

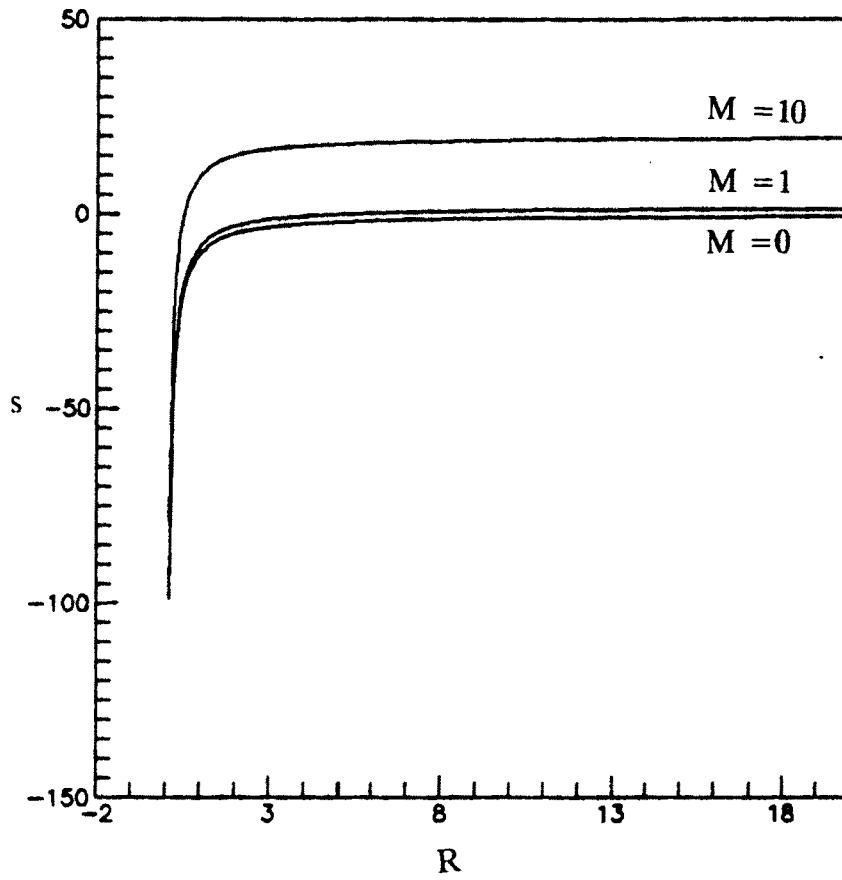


Fig. 5.16. Dependence of  $s$  on  $R$ ,  $m = 100.0$  (Mode c)

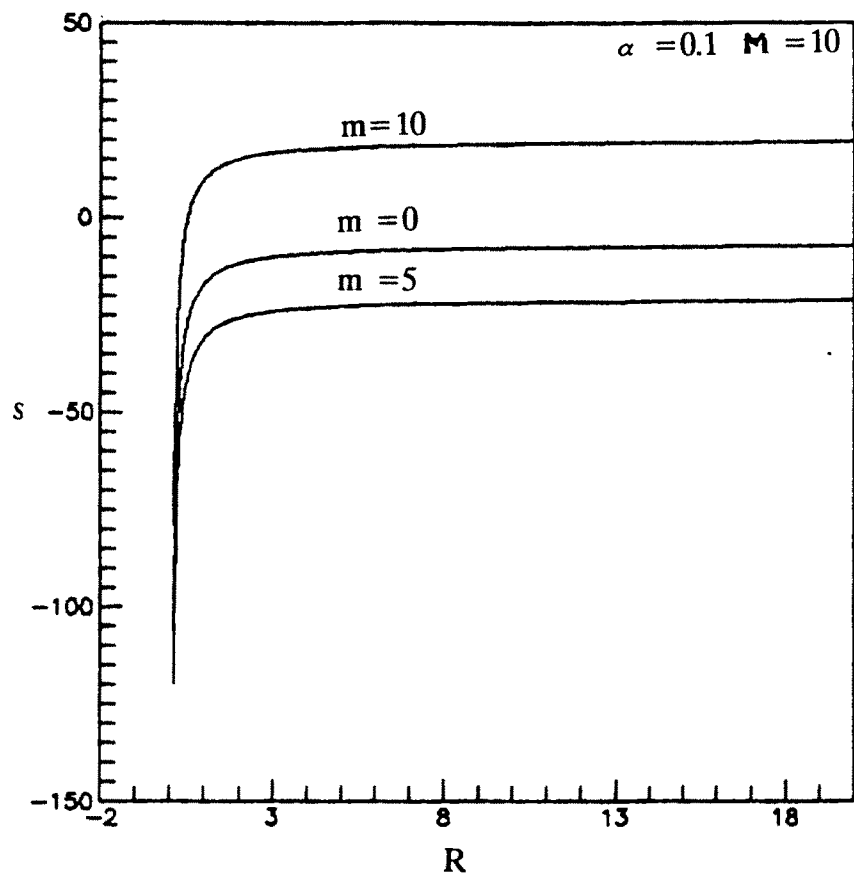


Fig. 5.17. Growth rates (Mode c) as function of the dimensionless variable  $R$ , for several values of  $R_m$

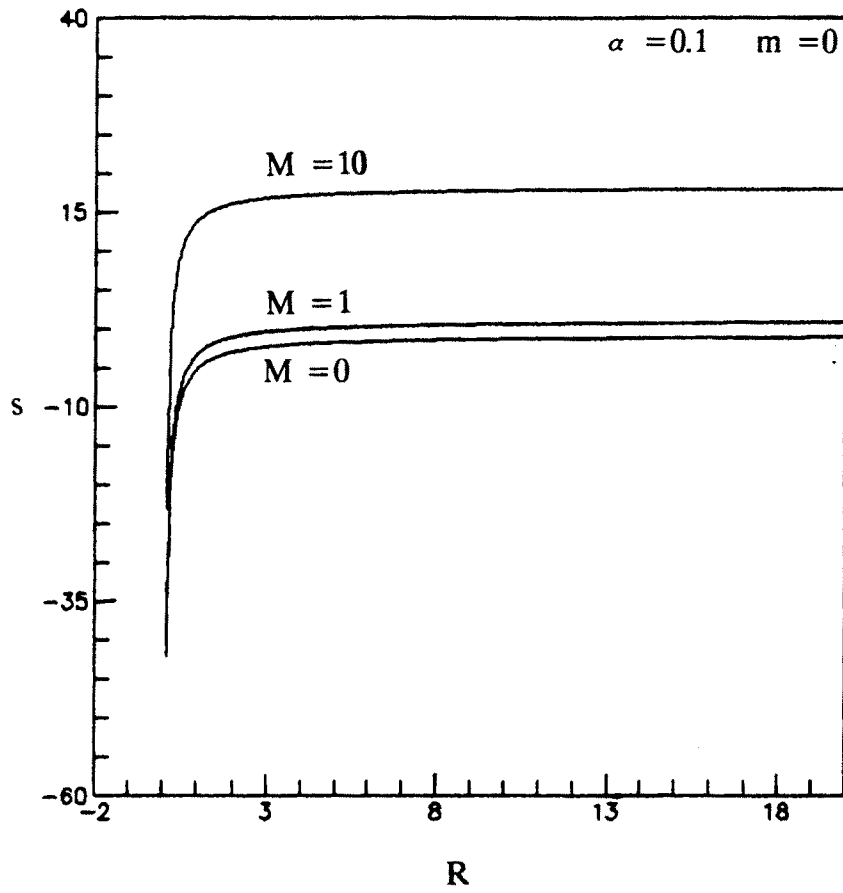


Fig. 5.18. Variation of  $s$  (Mode  $c$ ) with respect to  $R$  for various values of  $M$

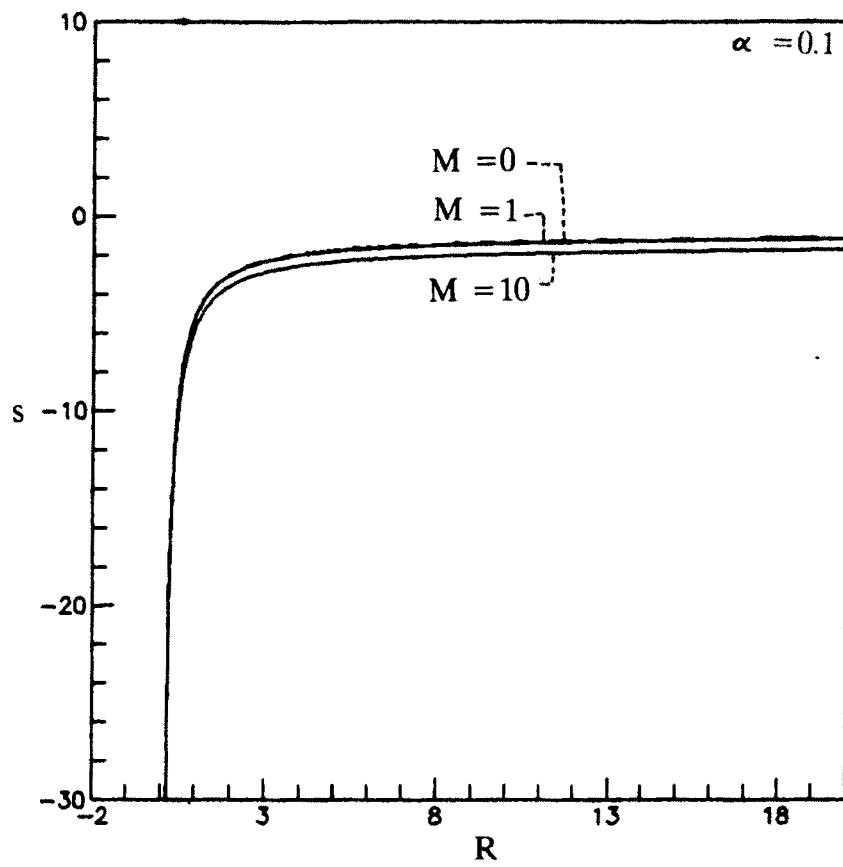


Fig. 5.19. Variation of the eigenvalues with respect to  $R$  for  $m = 10.0$  (Mode d)

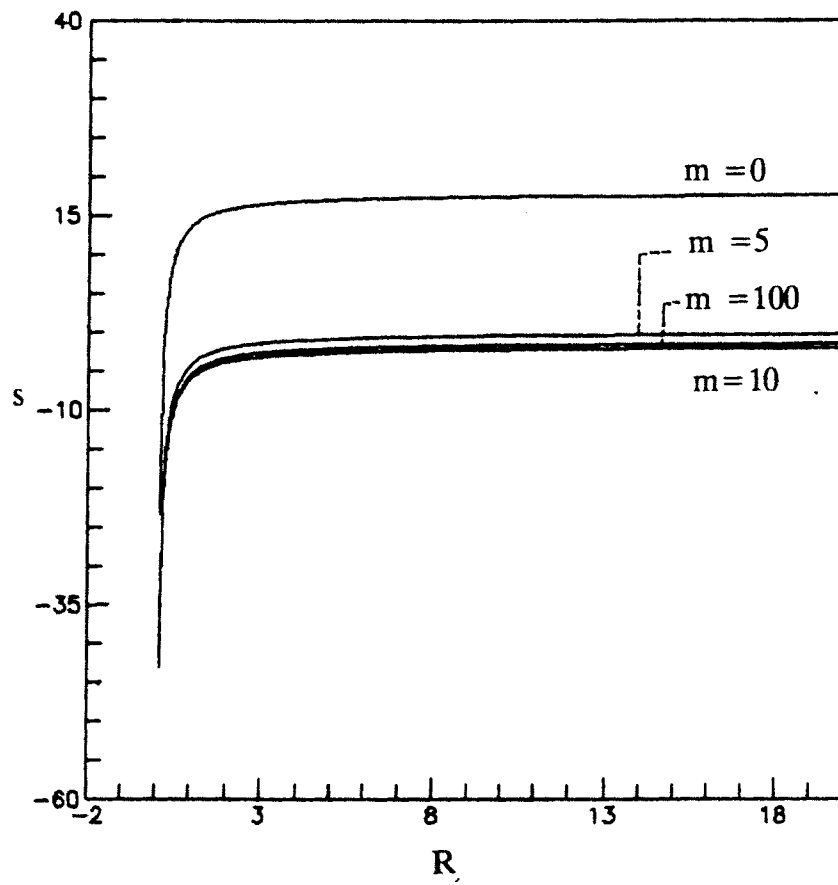


Fig. 5.20. Frequency distribution  $s$  for  $R$  when  $M = 10.0$  and  $\alpha = 0.5$  (Mode d)



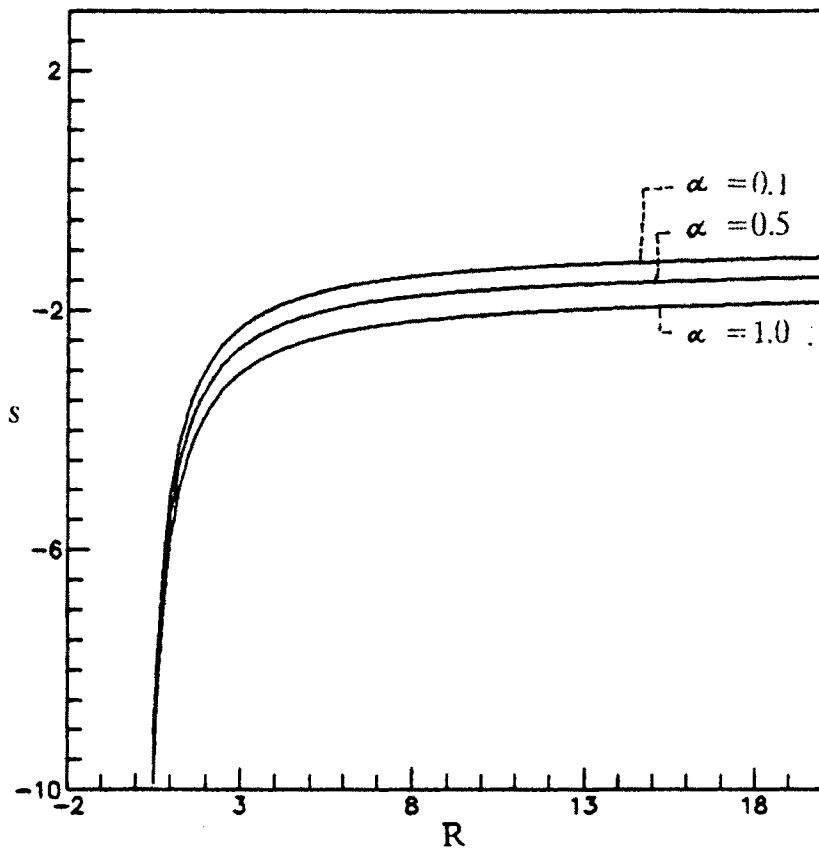


Fig. 5.21. Frequency distribution  $s$  for various values of  $\alpha$ ,  $m = 0.0$  (Mode d)

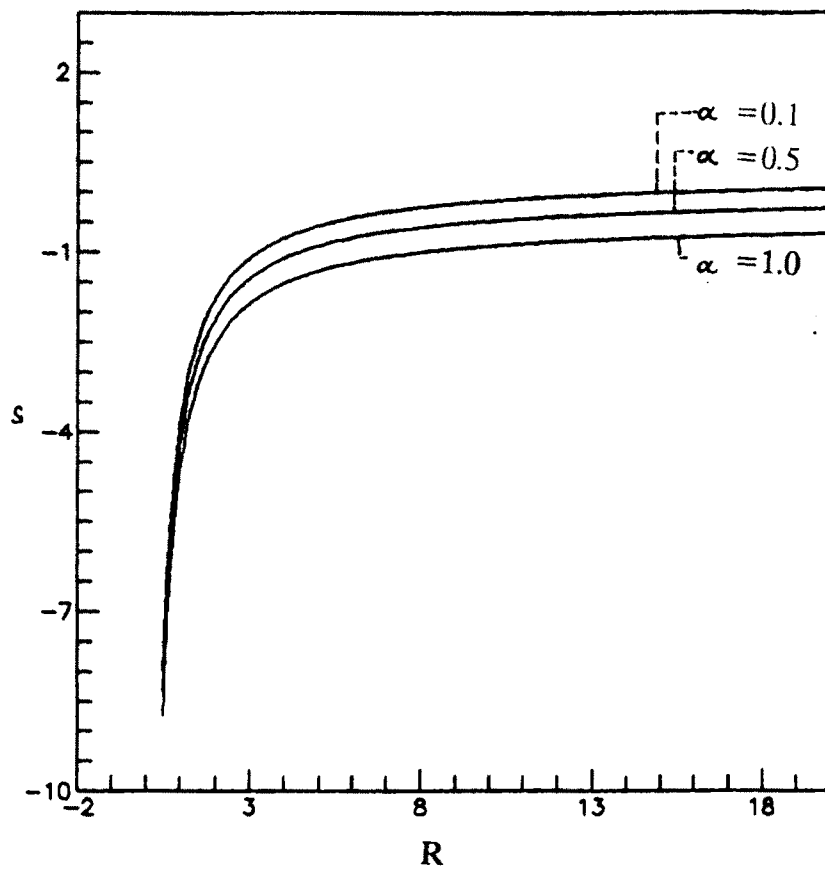


Fig. 5.22. Frequency distribution  $s$  for various values of  $\alpha$ ,  $m = 5.0$  (Mode d)